

# SYNTHESIS AND CHARACTERIZATION OF HIGH BELITE SULFOALUMINATE CEMENT THROUGH RICH ALUMINA FLY ASH AND DESULFURIZATION GYPSUM

BING MA, XUERUN LI, YUYI MAO, #XIAODONG SHEN

State Key Laboratory of Materials-oriented Chemical Engineering, College of Material Science and Engineering, Nanjing University of Technology, Nanjing 210009, PR China

#E-mail: myyanb@yahoo.cn

Submitted September 11, 2012; accepted April 4, 2013

**Keywords:** Industrial residue, Belite-sulfoaluminate, Fly ash, Desulfurization gypsum, Hydration

*The objective of this study was the preparation and characterization of high belite sulfoaluminate cement (HBSC) from industrial residues. HBSC promises eco-friendly building materials with great mechanical performance at earlier ages than Ordinary Portland Cement (OPC). Preliminary results show the formation of main phase dicalcium silicate ( $C_2S$ ) and ye'elimite ( $C_4A_3S$ ) at 1250°C, as determined by X-ray diffraction (XRD), are promising. The formation of minerals in the clinker was analyzed by differential scanning calorimetry-thermogravimetry (DSC-TG). Likewise, Scanning electron microscope (SEM) and XRD were used to carry out the analysis of the micro-structural and hydration products. The main HBSC hydration products, Ettringite and amorphous  $Al(OH)_3$ , were formed in the early stages; however, during the later stages, monosulfate and Strätlingite were formed. Isothermal conduction calorimetry measurements indicate that hydration properties of the cements are comparable to OPC; the total hydration heat after 3 days was 438 J/g. The optimum compressive strength values of the mortars after 1-, 3-, 7-, and 28-days were 24.9 MPa, 33.2 MPa, 35.6 MPa and 52.8 MPa which can meet the requirement of special structures.*

## INTRODUCTION

Energy conservation and emission reduction have become the modern world's current environmental protection themes. Pollution and the disposal of industrial wastes like fly ash (FA), desulfurization gypsum (FGD), and phosphogypsum have proven to be hot topics and seriously threaten subjects dealt with by scientists and technologists. In 2009, China's total fly ash output reached 3.75 million tons, while approximately 60 million tons worldwide came from coal combustion plants. Nowadays coal combustion plants have been equipped with flue gas desulphurization processes to produce desulfurized gypsum as well. Although FA and FGD are not classified as toxic waste hazards, there are concerns with trace elements, such as Cd, Hg, Pb, As, F, Ni, Pb, Cr and Se. Regularly, FA and FGD were piled in mounds for storage, where winds could raise dust and result in muddying the ambient particulate air. They are significant environmental pollutants that not only present a respiratory hazard when airborne, but also occupied land that contaminated the environment. Furthermore, many researchers have presented the critical content of fluoride in FGD (close to 150 mg/kg) was regarded as a destructive element [2, 3]. Excessive ingestion of fluoride in mammals can bring about fluorosis, affecting the teeth and skeletal tissues [4, 5]. Many epidemiological

studies have also associated exposure to small particles, like fine dust particles, resulting in lung cancer, heart-disease, asthma and increased mortality [6, 7].

It is commonly known that cement production is one of the most energy consuming processes, equal to the disposal of industrial by-products. Ordinary Portland Cement is composed of most man-made materials used worldwide, but it not only requires a mass of calcium-rich materials, but also requires high-temperature sintering for its formation, e.g. 1450°C. Consequently, the cement industry contributes around 6 % of all  $CO_2$  anthropogenic emissions [8, 9], which arose from calcite decarbonation.

Over the years, much attention has been paid to the development of modified cement clinkers, giving rise to energy preservation as well as interests concerning its use as a binder for waste encapsulation [10]. Sulfoaluminate cement (SAC) is based on high-belite cement by introducing  $C_4A_3S$ . One of such cements, including the major phases  $C_4A_3S$  (55-75 %),  $C_2S$  (8-37 %),  $C_4AF$  (3-10 %) and  $CaO \cdot SO_3(CS)$ , was developed and reported by a number of researchers [11-21]. Mehta [22] synthesized some modified Portland cement on the basis of a five component system: C-S-A-F-S. Sudoh etc. [23] synthesized another modified cement on the basis of a four component system: C-S-A-S. This can overcome the disadvantages of low mechanical strength developed

during early stages and all aforementioned research used bauxite as a raw material; this consumed a large amount of natural resources.

HBSC is the product of another idea based on sulfoaluminate cement, made by adjusting the proportions of  $C_2S$  and  $C_4A_3S$ , with nominal mineralogical compositions in the range  $C_2S$  (50-70 %),  $C_4A_3S$  (30-50 %), and aluminate phase. It can be formed at temperatures between 1200 ~ 1350°C. Usually, in this framework, 10 ~ 25 wt. % of gypsum is interground with the clinkers for an appropriate volume, setting, time, and intensity development [24].

Compared to traditional crafts, less attention has been paid to the use of desulfurization gypsum and fly ash. For the sake of this investigation, we tried our utmost to use industrial by-products, considering desulfurization gypsum has a similar physical and chemical performance to natural gypsum, and high-alumina fly ash has a satisfactory content of alumina oxide. We decided to use high-alumina fly ash instead of bauxite to make high belite-calcium sulfoaluminate cement, which allows us to use industrial solid waste and economy mineral resources.

## EXPERIMENTAL

### Raw materials

The raw materials were high-alumina fly ash and desulfurization gypsum from a Zhejiang plant, and limestone from Huaihai. The main oxide compositions of raw materials determined by chemical analysis are shown in Table 1.

### Samples preparation

The raw materials were ground in a laboratory ball mill to obtain fineness of 6-8 % over 80  $\mu\text{m}$  sieve. On the basis of required proportions, the raw meal was prepared by mixing the raw materials in proportion. The chemical composition of raw meal is shown in Table 2.

Table 1. Chemical composition of starting materials (wt. %).

Materials	LOI	CaO	SiO <sub>2</sub>	Al <sub>2</sub> O <sub>3</sub>	Fe <sub>2</sub> O <sub>3</sub>	SO <sub>3</sub>	MgO
Limestone	40.06	48.78	5.84	1.92	1.00	0.07	1.83
Fly ash	1.67	4.04	45.6	40.16	3.73	3.01	1.26
Desulfurization gypsum	24.94	34.01	–	0.90	0.19	39.96	–

LOI: loss of ignition

Table 2. Chemical composition of raw meal (wt. %).

CaO	SiO <sub>2</sub>	Al <sub>2</sub> O <sub>3</sub>	Fe <sub>2</sub> O <sub>3</sub>	SO <sub>3</sub>	LOI	C <sub>m</sub> <sup>a</sup>	P <sup>b</sup>	f-SO <sub>3</sub> <sup>c</sup>
36.71	15.14	11.21	0.69	3.78	29.52	0.988	2.96	1.41

a - basicity modulus, b - b-alumina sulfur modulus, c - free sulfur trioxide

The raw meal was mixed with water and pressed with a pressure of 15 MPa into disk mold of  $\Phi$  40mm  $\times$  25 mm. The disks were dried in the stove, then calcined in a Si-Mo rod resistance furnace at different temperatures (1200, 1250, 1280, 1300, 1320, 1350°C for 30 min, removed from the furnace at once and cooled rapidly by fan. Clinker samples were all ground to pass through an 80  $\mu\text{m}$  sieve. Some dried wafers were fired at the same temperature (1250°C) for 30, 60, 90 and 150 min respectively, then removed from the furnace and cooled rapidly by a fan. The emblematic firing schedule is present in Figure 1. The clinkers were relatively soft and friable to OPC; consequently, the whole process brought about considerable energy conservation.

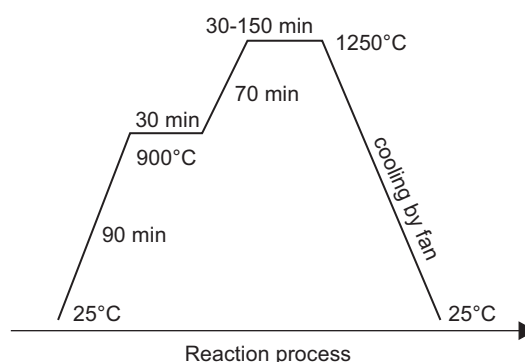


Figure 1. Schematic diagram of firing profile for the clinker preparation.

### Characterization

In order to investigate clinker formation at different temperatures, the content of free lime in the clinkers was determined chemically after dissolving the clinker with ethanol-glycol. The mineral compositions of the clinkers burned at different temperatures, and were analyzed by X-ray diffraction (ThermoFisher ARL 9900 series X-ray workstation using Co K $\alpha$  radiation,  $\lambda = 0.1788996$  nm).

Hydration heat release of HBSC was determined by a conduction calorimeter (Thermometric TAM Air). The microstructures of the samples were observed with a scanning electron microscope and energy dispersion spectroscopy (SEM-EDS) (Model JSM-5900) and XRD. Hydration products at different ages were determined by XRD and DSC-TG.

## RESULT AND DISCUSSION

### The burn ability of the clinker

The contents of f-CaO in samples burned at different temperatures are shown in Table 3. It can be seen that the free lime contents of the clinkers at different temperatures were all low, which indicates that raw materials were calcined completely from 1250°C.

Table 3. The content of f-CaO in samples burned at different temperature (wt. %).

Temperature (°C)	1250	1280	1300	1320	1350
f-CaO (%)	0.081	0.079	0.082	0.080	0.084

The clinker phase composition estimated by a K value method is shown in Table 4. Note that the belite phase was mostly present as the  $\beta$  modification, but the value given in Table 4 represents the sum of all of the different belite polymorphs detected.

Table 4. Measured phase composition of the clinker.

Phase	Belite	Ye'elimite	Calcium Aluminum Oxide
Mass %	56.2	34.4	7.4

### The formation condition of clinkers

The changes of solid phase composition with ongoing formations at different temperatures were determined by XRD was shown in Figure 2. As shown in Figure 2, the firing products of HBSC are mainly  $C_2S$ ,  $C_4A_3S$ ,  $C_3A$ , microscale of ferrite ( $C_4AF$ ) and mayenite ( $C_{12}A_7$ ). It shows that the diffraction patterns correspond to a basic clinker. The major phases of belite and calcium sulfoaluminate were well crystallized; moreover, the quantitative phase analysis (QPA) measured mineral content, which is shown in Table 4. From the XRD analysis, we can see the clinker formation in different temperatures; at 1250°C nothing has changed, but at 1200°C we can clearly see the clinker had not formed completely; it had parts of free calcia. When the raw meal is burnt at 1200°C f-CaO is found in XRD pattern, which indicates the raw meal is not burnt completely. As the burning temperature reaches 1250°C the content of f-CaO reduces sharply whilst the content of calcium

sulfoaluminate and belite increase markedly since the f-CaO participates in the chemical reaction to form calcium sulfoaluminate and belite. After the burning temperature exceeds 1350°C the contents of minerals remain constant, which suggests that the raw meal is burnt thoroughly after 1250°C. From Figure 3, we see phase content remained unchanged as the soaking time increased; the shape of the peaks show no change during soaking times exceeding 0.5 h. This reveals that the clinker formation mechanisms were irrelevant to soaking times, and it can conclude that HBSC can be prepared completely at 1250°C with no need for soaking.

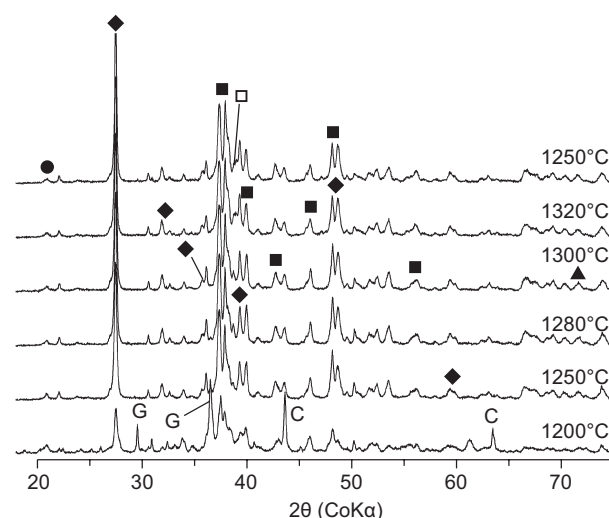


Figure 2. XRD patterns of sample burned at different temperatures ( $\blacklozenge$  -  $C_4A_3S$ ,  $\blacksquare$  -  $C_2S$ ,  $\blacktriangle$  -  $C_4AF$ ,  $\bullet$  -  $C_{12}A_7$ ,  $\square$  -  $C_3A$ , C - CaO, G - Gypsum).

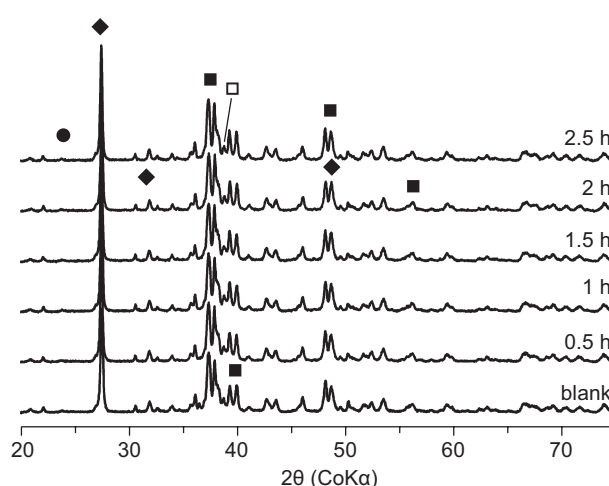


Figure 3. XRD patterns of sample burned at 1250°C for different soaking times ( $\blacklozenge$  -  $C_4A_3S$ ,  $\blacksquare$  -  $C_2S$ ,  $\square$  -  $C_3A$ ,  $\bullet$  -  $C_{12}A_7$ ).

### DSC-TG analysis for the clinker formation mechanisms

Figure 4 A and B show the DSC and TG curves for the HBSC clinker formation. Figure 4 B shows decarbonation as the main weight loss. As expected,

Figure 4 A displays a number of thermal effects. Two strong endothermic peaks corresponding to a weight loss resulting from the dehydration of the gypsum and the decomposition of  $\text{CaCO}_3$ , are observed at  $125.1^\circ\text{C}$  and  $795.9^\circ\text{C}$ , respectively (points P1 and P2). The experimental values of weight loss were 1.84 and 28.33 wt. % respectively. The small endothermic peak at  $856.5^\circ\text{C}$  (point P3), is associated with the beginning of ye'elimite formation. The sharp exothermic peak at  $1301^\circ\text{C}$  (point P4) corresponds to the rapid formation of ye'elimite. Finally, the TG curve is part of a large downward trend due to partial melting of the aluminate phases and also to the ye'elimite partial decomposition (starting from point P5) [25-26].

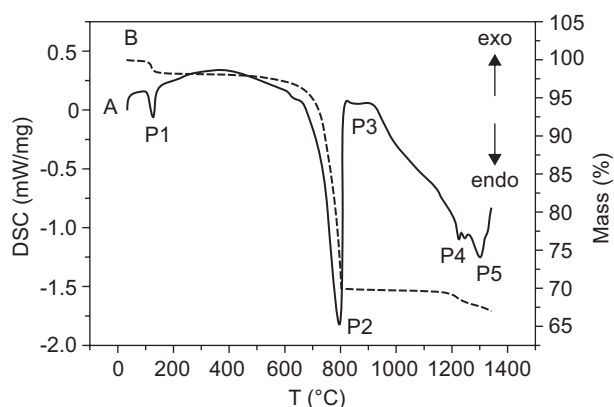


Figure 4. DSC–TG curves of HBSC clinker formation.

#### Isothermal calorimetry

The results of conduction calorimetry are given in Figure 5. A conduction calorimeter was used to confirm the rate of hydration heat released during the first three days. HBSC has a transition point after the initial peak until a sample age of about 4 h; after that, it has another hydration peak at 10 h. A second maximum heat flow takes place after 26.4 h. The gross total hydration heat after 3 days for HBSC is 438 J/g. Compared to the OPC clinker, which was 227 J/g, hydration heat release

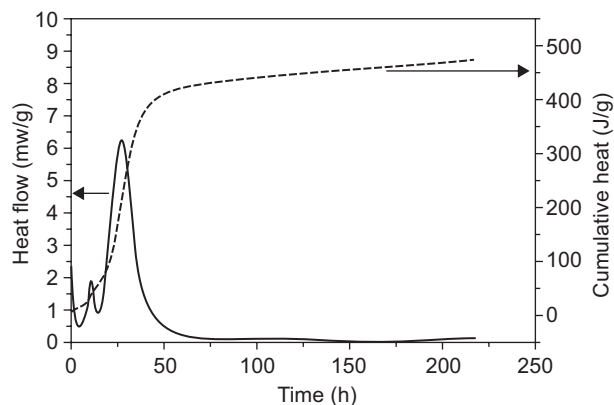


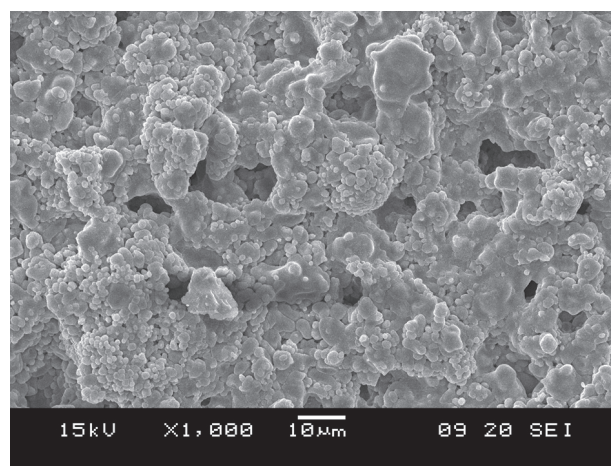
Figure 5. Isothermal conduction calorimetry of HBSC cement.

of HBSC was much higher than OPC at early ages. It reveals that HBSC is more reactive with water, which indicates the high performance at early stages.

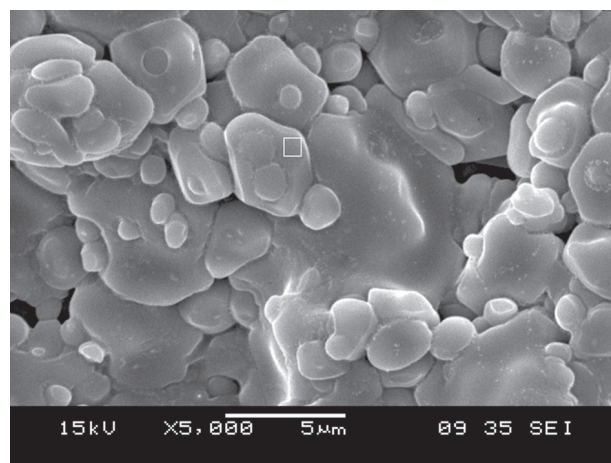
#### Morphology analysis

##### Clinker

Figure 6 shows the SEM-EDS images of a cement clinker. From Figure 6b, it is clear that there were many with a hexagonal plate shape, which was  $\text{C}_4\text{A}_3\text{S}$ ; irregular round granules were  $\text{C}_2\text{S}$ . Meanwhile, Figure 6a revealed a HBSC clinker had high porosity results in grindability and enough superficial area to react with water.



a) 15 kV × 1000



b) 15 kV × 5000

Figure 6. SEM photographs and EDS patterns of cement clinker at different magnify multiple.

#### Hydration of sample XRD analysis

The hydration of cement in order to determine the composition of solids and liquids after different stages was determined by XRD and DSC. From Figure 7, it can be clearly seen that after 2 h ye'elimite and gypsum both consumed, and ettringite had formed as a new crystalline phase, according to Equation 1. After 10 h

of hydration, traces of monosulfate and crystalline gibbsite are detectable, while gypsum has almost been depleted, according to Equation 2. After hydration of 2d, strätlingite formed from  $C_2S$  as a silicon source and  $AH_3$  as an alumina source to react according to Equation 3.

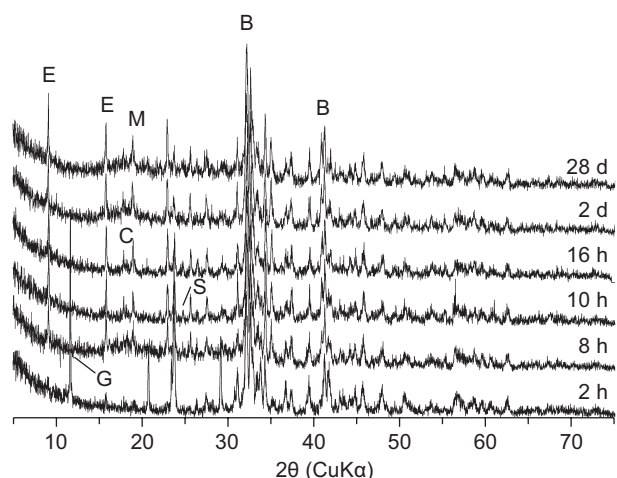
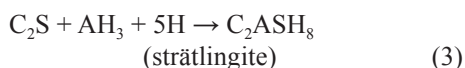
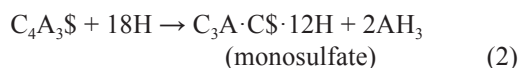
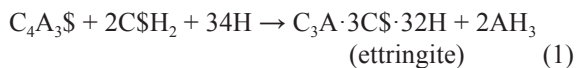


Figure 7. XRD patterns of the sample hydrated after 2, 8, 10, 16 h, 2, 28 d at  $w/c = 0.39$ .

### DSC analysis

The XRD results are also verified by the DSC data (Figure 8). From the figure it is revealed that weight loss increased with ongoing hydration time at 90-150°C, which was a result from the increased ettringite. Four hours of hydration consumed a part of gypsum (weight

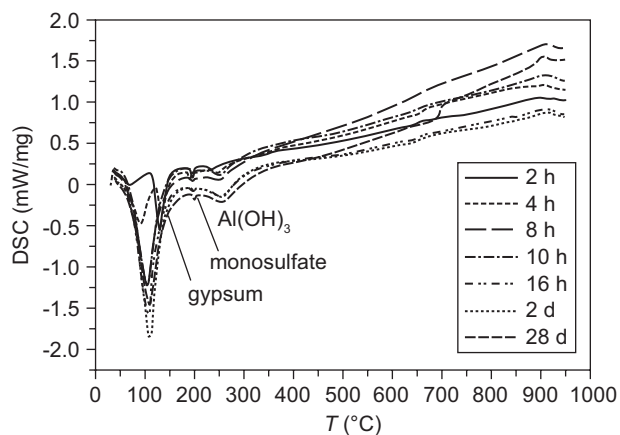


Figure 8. DSC analysis of sample hydrated after 2, 4, 8, 10, 16 h, 2, 28 d at  $w/c = 0.39$ .

loss at around 150°C) and formed some  $Al(OH)_3$  (weight loss at about 300°C). After 10 h, ettringite formation was mostly completed, and monosulfate begin to form (weight loss at about 190°C). From the XRD analysis, the ettringite content stayed constant after 16h. Monosulfate traces were detectable after 10 h of hydration.  $Al(OH)_3$  formed continuously as an additional hydration product. HBSC showed almost no increase of  $Al(OH)_3$  beyond the hydration time of 2 days. This can be explained by the fact that  $Al(OH)_3$  was consumed by the formation of strätlingite, as the present belite started to take part in the hydration process after 2 days. The strätlingite formed can be identified in the sample hydrated for 2 days (weight loss at about 170°C).

### SEM analysis

The SEM experiment was performed to observe the surface topography of hydrated samples at different stages. As shown in Figure 9, the more needle-shape and columnar ettringite (AFt) was among the hydration products of the HBSC. After 10 h of hydration, the flake-like monosulfate formations are visible. The pores in the hardened cement pastes are filled with well-developed AFt, and the hardened cement paste is a coarse-grained slurry. In addition, there was also evidence of gelatinous calcium silicate hydrates. These hydration products linked with each other and formed a dense, net-shaped structure.

### Compressive strength measurement

In order to determine the optimum content of gypsum in the belite-sulfoaluminate cement, HBSC was produced in the laboratory by mixing clinkers (density 2.92  $g/cm^3$ , Blaine surface area 357  $m^2/kg$ ) with varied gypsum. The 1-, 3-, 7-, and 28-day curing ages of mortar compressive strength were measured on 40mm×40mm×160mm cubes. The water/cement and sand/cement ratios were kept at 0.5 and 3, respectively, for all the HBSC. The compressive strength results are listed in Table 5. Additionally, we compared the two different clinkers of compressive strength, HBSC and OPC, shown in Figure 10. It can be clearly seen that the compressive strength of HBSC is comparable to OPC at 28 days. Especially important features of the two cements were their differing hydration mechanisms. During the early hydration stage, formation of ettringite leads to strength development in HBSC, while C-S-H develops in OPC. In later stages, the strength development of HBSC mainly depends on C-S-H gel formation [27]. The strength of mortar on 90 days and 180 days are 63.6 MPa and 74.4 MPa, respectively. Compared with the strength on 28 days, the long term strength increases steadily. Thus the performance of such cement can meet the requirements of special projects. From the compressive strength of 3d and 28d, meanwhile, we can conclude the optimum content of gypsum was 15 %.

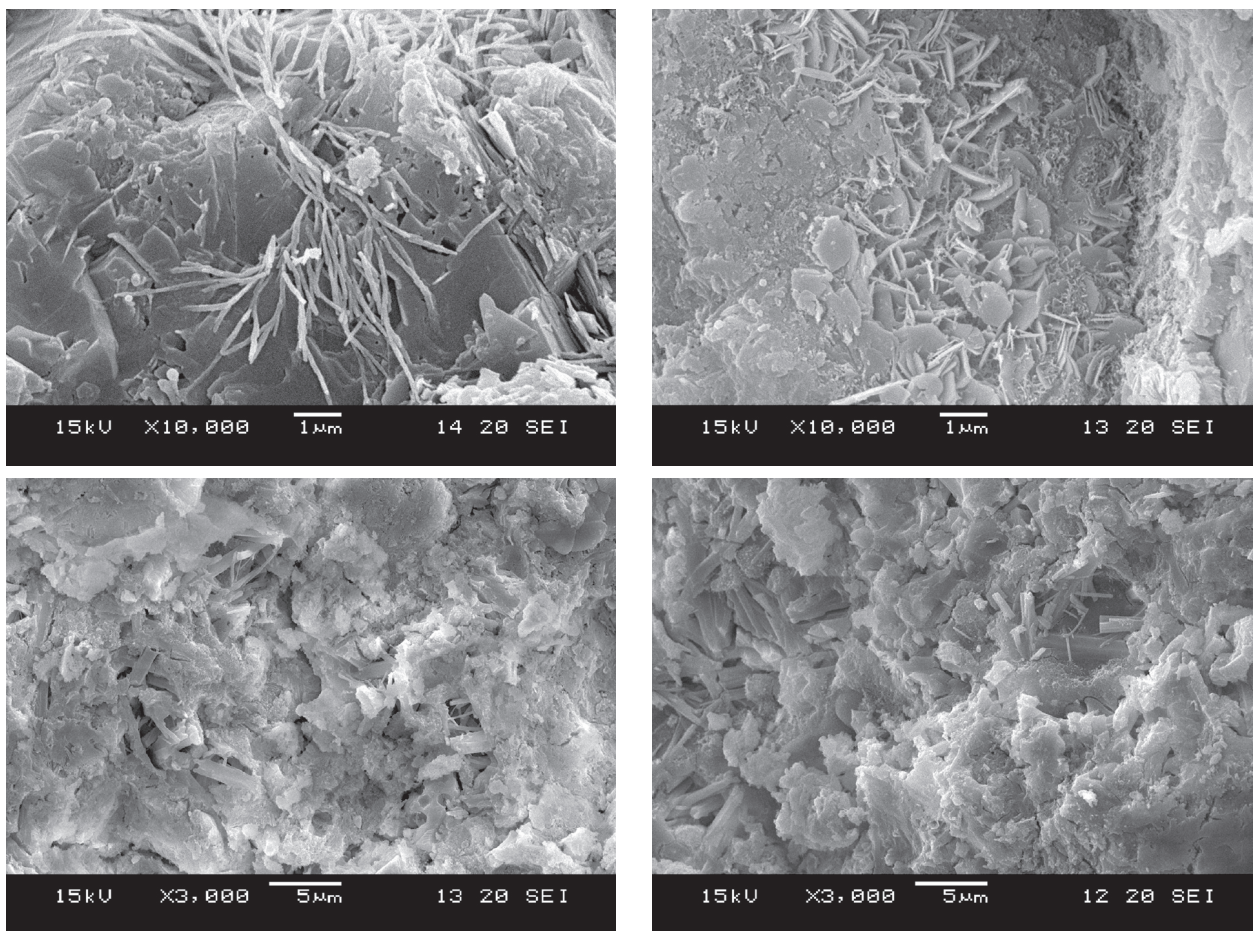


Figure 9. SEM image of cement hydrated for different ages.

Table 5. Compressive strength of HBSC with varied gypsum.

Number	1d	3d	7d	28d
5 %	17.1	24.2	24.7	33.4
8 %	20.2	27.4	28.1	41.4
10 %	27.6	30.5	33.2	44.8
15 %	24.9	33.2	35.6	50.8
20 %	21.2	28.4	30.2	48.7

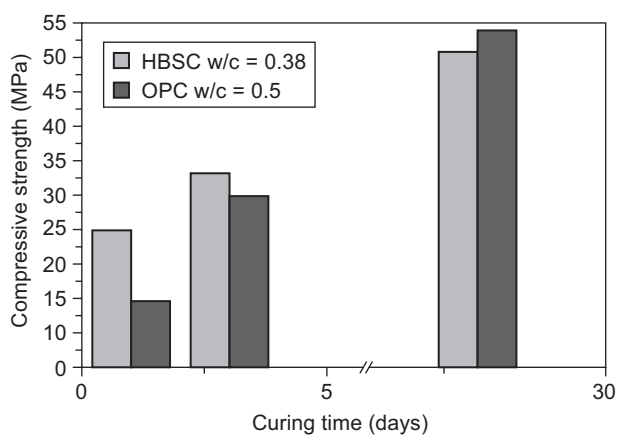


Figure 10. Compressive strength of HBSC (gypsum: 15 %) and OPC.

## CONCLUSIONS

- Utilization of industrial solid wastes like high-alumina fly ash and desulfurization gypsum can synthesize high belite sulfoaluminate cement at around 1250°C and without for soaking, contrary to other literature which states the temperatures were higher and there was a need for soaking a period of time. Besides that, fly ash and FGD can account for 40 % approximately in raw material dosing.
- The main hydration products of HBSC in early stages are ettringite and amorphous  $Al(OH)_3$ ; afterwards, monosulfate is formed as well as strätlingite. Ettringite contributes to the development of early strength.
- Microstructural evaluations and compressive strength indicate the usefulness of this type cement, which meet special engineering requirements.
- Utilization of industrial solid wastes with especially high alumina contents of fly ash, which can ease the shortage of bauxite resources pressure, provide a new way to synthesize high belite sulfoaluminate cement.

Acknowledgments

The authors gratefully acknowledge the financial supports from the National Basic Research Program of China (No. 2009CB623100); the Natural Science Fund for colleges and universities in the Jiangsu Province (No.08KJB430006); Open Fund for the Key Laboratory of Inorganic and Composite Materials in Jiangsu Province (No.wjjqfhhxc1200801) and the Specialized Research Fund for the Doctoral Program of Higher Education of China (20093221120010) and Thermofisher ARL 9900 series X-ray workstation.

REFERENCES

1. Johnson J.: J. Am. Chem. Soc. 87, 44(2009).
2. Alvarez-Ayuso E., Querol X., Tomas A.: J. Hazard. Mater. 153, 544 (2008).
3. Alvarez-Ayuso E., Querol X., Tomas A.: Chemosphere. 65, 2009 (2006).
4. Meenakshi, Maheshwari R.C.: J. Hazard. Mater. 137, 456 (2006).
5. Heikens A.: Sci. Total Environ. 346, 56 (2005).
6. Zanobetti A., Schwartz J.: Environ. Health Perspect. 115, 769 (2007).
7. Knox E.G.: J. Epidemiol. Community Health. 62, 442 (2008).
8. Damtoft J.S., Lukasik J., Herfort D., Sorrentino D., Gartner E.M.: Cem. Concr. Res. 38, 115 (2008).
9. Gartner E.: Cem. Concr. Res. 34, 1489 (2004).
10. Mehta P.K.: World Cem. Technol. 11, 166 (1991).
11. Peysson S., Pera J., Chabannet M.: Cem. Concr. Res. 35, 2261(2005).
12. Arjunan P., Silsbee M.R., Roy D.M.: Cem. Concr. Res. 29, 1305 (1999).
13. Drissi M., Diouri A., Damidot D., Greneche J.M., Taibi M., Taibi M.A., Taibi M.: Cem. Concr. Res. 40, 1314 (2010).
14. Martin-Sedeno M.C., Cuberos A.J.M., Dela Torre A.G., Alvarez-Pinazo G., Ordonez L.M., Gateshki M., Aranda M.A.G.: Cem. Concr. Res. 40, 359 (2010).
15. Juenger M.C.G., Winnefeld F., Provis J.L., Ideker J.H.: Cem. Concr. Res. 41, 1232 (2011).
16. Keith Q.: Cem. Concr. Res. 31, 1341 (2001).
17. Pera J., Ambroise J.: Cem. Concr. Res. 34, 671 (2004).
18. Janotka L.K.I.: Bull. Mater. Sci. 23, 521 (2000).
19. Li H.X., Agrawal D.K., Cheng J.P., Silsbee M.R.: Cem. Concr. Res. 31, 1257 (2011).
20. Coumes C.C.D., Courtois S., Peysson S., Ambroise J., Pera J.: Cem. Concr. Res. 39, 740 (2009).
21. Luz C.A., Rocha J.C., Cheriaf M., Pera J.: J. Hazard. Mater. 136, 837 (2006).
22. Mehta P.K.: World Cem. Technol. 21, 166 (1980).
23. Sudoh G., Ohta T., Harada. in: Proceedings of the 7<sup>th</sup> International Cong. Chem. Cem. 3, p. 152, 1980.
24. Glasser F.P., Zhang L.: Cem. Concr. Res. 21, 1881 (2001).
25. Ma S.H., Shen X.D., Gong X.P., Zhong B.Q.: Cem. Concr. Res. 36, 1784 (2006).
26. Ma S.H., Shen X.D., Huang Y.P., Zhong B.Q.: J. Chinese. Cera. Soci. 36, 1 (2008).
27. Taylor F. W.: Cem. Chem. London, 1990.